Sustainable Materials and Technologies 29 (2021) e00295

Contents lists available at ScienceDirect

Sustainable Materials and Technologies

journal homepage: www.elsevier.com/locate/susmat

Effect of waste PET and CR as sand replacement on the durability and acoustical properties of semi dense asphalt (SDA) mixtures

Peter Mikhailenko [a,*], Zhengyin Piao [a,b], Muhammad Rafiq Kakar [a,c], Sahand Athari [d], Moises Bueno [a], Lily D. Poulikakos [a]

[a] Empa, Swiss Federal Laboratories for Materials Science and Technology, Laboratory for Concrete and Asphalt, Dübendorf, Switzerland
[b] ETH Zurich, Swiss Federal Institute of Technology Zurich, Institute of Environmental Engineering, Ecological Systems Design, Zurich, Switzerland
[c] Bern University of Appllied Sciences, Department of Architecture, Wood and Civil Engineering, Bern, Switzerland
[d] Empa, Swiss Federal Laboratories for Materials Science and Technology, Laboratory for Acoustics/Noise Control, Dübendorf, Switzerland

ARTICLE INFO

Article history:
Received 21 December 2020
Received in revised form 22 March 2021
Accepted 17 May 2021

Keywords:
Asphalt pavement
Crumb rubber (CR)
Polyethylene terephthalate (PET)
Water sensitivity
Sound absorption
Semi-circular bending

ABSTRACT

Construction materials research is consistently striving to improve sustainability, in the reduction of virgin materials by use of otherwise landfilled materials of the same purpose. Crumb rubber (CR) from end-of-life tires and polyethylene terephthalate (PET) from post-consumer liquid containers are two of the most commonly circulating forms of waste in the urban environment. This study investigated the replacement of semi-dense asphalt (SDA) sand by untreated mechanically shredded CR and PET, at 2.5 and 5.1% respectively by total mass of aggregates. The mixtures were evaluated by compactability, indirect tensile strength (ITS), fracture energy (FE), water sensitivity by ITS ratio (ITSR%), surface texture and acoustic absorption tests. After compaction, the CR and PET samples experienced an elastic rebound effect, which resulted in the air voids being higher than expected. Also, the PET samples required more compaction energy. The ITS, FE and ITSR% were significantly reduced with CR replacement, while the PET mixture performed similar to the control, especially in FE. The sound absorption was related more to the air voids than the material type, although the absorption coefficients of the SDA was not found to be significant. The CR reduced the texture level of the pavement significantly in comparison to the control, while texture level remained the same for the PET mixture, despite a difference in the porosity. Further studies were performed using a mixture replacing PET by aggregate volume at 5.1%, comparing it to the control SDA in terms of low temperature cracking and permanent deformation at 50 °C. While the compactability of the PET mixture was now similar to that of the control, the resistance to cracking and permanent deformation was lower. Although the PET mixture had some interesting ductility properties, the replacement of sand by CR and PET is not recommended, and the more common use as asphalt mixture modifiers with fairly low addition contents of around 1% is more sound.

1. Introduction

With increases in demand, the fabrication of construction sand is a significant challenge for construction materials going forward [1]. The sand in asphalt pavement mixtures is made by crushing quarried larger sized aggregates. The use of marginal waste materials could partially address this issue while providing a useful destination for waste materials [2]. Among these materials are crumb rubber (CR) or polyethylene terephthalate (PET) flakes, which are waste materials with a particle size similar to sand and melting point compatible with hot mix asphalt. Furthermore, they are abundant in the urban environment [3].

CR is sourced from end of life tires (ELT), and has been used in asphalt mixtures since the 19th century [4]. Out of the estimated 3 Mt. of ELT collected in the EU each year, it is estimated that 1.2 Mt. are landfilled [3]. After vehicle tires are too worn to be safe and to be recycled into new tires, they can be broken down to produce CR [5]. The rubber is processed to reduce the particle size and sometimes treated or pre-swelled. The CR can then be incorporated into the asphalt mixture in two ways: i) during the asphalt mixing added to hot aggregates known as the dry process [6] or ii) pre-mixed with the asphalt binder used in the mixture known as the wet process [7] including terminal blend, which is done at higher temperatures [8]. The replacement of asphalt sand by CR would constitute a type of dry process.

The mechanical characteristics of CR dry process modified asphalt mixture compared to conventional mixtures have been mixed, as some studies showed improved fatigue resistance [9,10], while others showed it decreased [11]. The rutting resistance of the mixture was not found to

* Corresponding author at: Concrete and Asphalt Laboratory, Empa, 129 Ueberlandstrasse, 8600 Dübendorf, Switzerland.
E-mail address: peter.mikhailenko@empa.ch (P. Mikhailenko).

https://doi.org/10.1016/j.susmat.2021.e00295

be altered significantly [9], or improved with CR [12]. Furthermore, the indirect tensile strength ratio (ITSR%) from water sensitivity was found to not change significantly [13] or decrease [11,14]. The addition of various additives to CR has been shown to improve these asphalt mixture properties [3]. In addition to the mechanical performance, the sounds absorption properties were shown to be not very different [15], while the surface texture was found to be smoother with CR [16,17].

PET waste comes primarily from discarded plastic bottles and other plastic containers [2,18]. The PET recycling rate can be as much as 82% for places like Switzerland [19], but it is less than half in other countries [20]. Asphalt mixture can be a destination for this waste. While studies using PET modified binder exist [21–27] – including its application in the field [28] – their relatively high melting point compared to other waste plastics and bitumen, it has been primarily incorporated using the dry process. This is also less conducive to consuming large volumes of PET given the binder represents 4–7% of asphalt mixtures.

The performance of asphalt mixtures modified with PET has been promising with studies showing improved fatigue [29–31], rutting resistance and resistance to permanent deformation [32,33], binder drain down [34], as well as the moisture sensitivity by indirect tensile strength ratio (ITSR%) [35]. However, this is generally only up to 1% by weight of the mixture, and higher rates would reduce this performance. These are promising results and show that the incorporation of PET into different types of asphalt mixtures warrants further investigation.

Several studies have already attempted to use PET as aggregates in dense asphalt mixtures. They have found a reduction in the stiffness [36–38], tensile strength and low temperature cracking susceptibility [39]. However, the moisture sensitivity and rutting was found to improve [13,38].

Given that CR and PET have shown some interesting results as additives to asphalt mixtures, their ability to replace the sand in higher porosity mixtures is of interest. In this study semi-dense asphalt (SDA) mixtures with CR and PET replacement of the sand fraction were investigated. Initially, two trial mixes incorporating each material were produced and tested for volumetrics, compactability, indirect tensile strength (ITS) and water sensitivity. Additionally, these mixes were tested for their sound absorption and texture properties. Based on the results, an improved PET mixture was produced and tested for crack and permanent deformation resistance against the control.

2. Materials and testing

2.1. Materials

2.1.1. Bitumen and aggregates

The binder used for the asphalt mixture was an SBS (styrene-butadiene-styrene) polymer modified binder (PmB) graded at 45/80 – 65 according to the penetration EN 1426 [40] and softening point (EN 1427). The control aggregates were quarried sandstone from FAMSA (Switzerland). The mixture used for this testing was Semi-Dense Asphalt (SDA 4–16), currently a commonly used gap graded mixture in Switzerland, primarily used for its low-noise properties [41]. Polymer modified binder is part of the requirements for SDA in the Swiss standards SN 640 436 [42]. The maximum aggregate size was 4 mm and the required air voids content was 16 ± 2%. It should also be noted that the binder is the same for all of the mixtures, allowing the effect of sand replacement to be distinguished.

The waste materials (Fig. 1) were selected for their compatibility as a sand fraction (particle size mostly between 0.1 and 2 mm), and their availability in the waste stream. The CR and PET were both untreated and their densities were about half the density of the sandstone (Table 1). The CR was produced by Tyre Recycling Solutions (Switzerland) through the mechanical grinding of waste truck tires, with no further treatment, making them relatively cheaper to treated CR types [7] and more viable for higher volume replacement. The metal content was 0.011%, which is in the typical range of CRs [7]. CR being a vulcanized material, cannot melt and flow due to its crosslinked nature, this is why they are so challenging to recycle. Therefore, rubber crumbs do not have a melting temperature; when heated they will start degrading at a temperature above 200–250 °C, and so can be used as aggregates.

The PET was sourced from RecyPET (Switzerland), and is mostly from recycled plastic bottles, delivered in the form of flakes. This could be classified as “crumb PET”. Since flaky particles are mostly found at higher aggregate sizes [43], this replacement is expected to change the overall aggregate shape profile. The high melting temperature of PET indicated that they will not melt during the asphalt mixture production process.

The gradations for the control and waste aggregates are shown in Table 2. The SDA 4–16 mixture comes in three fractions, the coarse aggregate, sand and filler, which makes the sand replacement simpler. The CR is fine compared to the sand, with most particles 0.125–1 mm. The PET is more coarse than CR, having most particles between 0.5 and 2 mm. The narrow gradation of CR and PET limits the amount of sand that can be replaced while keeping the gradation within the limits for the mixture.

2.1.2. Asphalt mixtures

The mixture compositions are shown in Table 3. In the initial two mixtures with waste materials, the CR and PET replaced the sand fraction by mass at 2.5 and 5.1% by the total mass of the mixture, respectively. The replacement levels were close to the highest successful replacement rates found in previous studies. Based on the results in the first two mixtures (see Results and Discussion), another PET mixture was produced where the PET was replaced by its volume relative to the sandstone, meaning the PET content was about half of the initial mixture due to its lower density (see Table 1). The binder content was increased to 6.1% to improve compactability and compared to a control mixture with the same binder content. The second set of experiments were designed to determine the low temperature (0 °C) and intermediate temperature (50 °C) behavior of the material were susceptibility for cracking and rutting could exist.

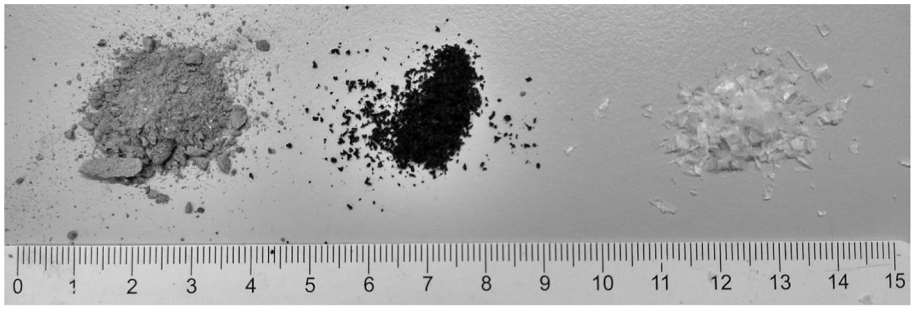

Fig. 1. Waste materials for aggregate replacement: control sand (left), CR (middle) and PET (right).

Table 1
Physical properties of aggregates and waste materials.

Aggregate Fraction	Apparent Density Mg/m^3	Bulk Density	Melting Temperature (°C)[a] °C	Glass Transition Temperature (°C)[a] °C	TGA % mass @800°C[b] %
2/4 Coarse	2.711	2.647	–	–	–
0.063/4 Sand	2.699	2.657	–	–	–
0/0.063 Filler	2.729	–	–	–	–
CR	1.270	–	–	−18 to −25	7
PET	1.416	–	245.6	81	14

[a] Found by differential scanning calorimetry (DSC).
[b] Thermogravimetric analysis % of original mass remaining.

Table 2
Gradation of aggregates and waste materials (by mass).

%Passing	Control Sandstone			CR	PET
Sieve Size (mm)	2/4	0.063/4	0/0.063		
8.0	100.0	100.0	100.0	100.0	100.0
5.6	99.8	100.0	100.0	100.0	100.0
4.0	73.9	97.4	100.0	100.0	99.9
2.8	26.3	87.1	100.0	100.0	99.5
2.0	5.0	77.7	100.0	100.0	96.2
1.4	0.8	64.9	100.0	100.0	38.4
1.0	0.6	52.0	100.0	100.0	24.6
0.500	0.5	35.8	100.0	82.0	8.2
0.250	0.4	24.6	100.0	35.0	2.3
0.125	0.3	11.2	98.0	9.0	1.3
0.063	0.1	3.7	82.0	2.0	1.2

The mineral aggregates were heated to a temperature of 170 °C before mixing, while the waste aggregates were not pre-heated. The aggregates mixed in the drum for 5 min, with another 4.5 min of full mixing after the introduction of the binder.

2.2. Testing

2.2.1. Volumetrics and compaction

The maximum relative density of the loose mixture was determined by EN 12697-5 from five samples for each mixture. Asphalt mixture cylinders were then compacted by gyratory compactor at a temperature of 155 °C to 16 ± 2% air voids. The samples were kept at 155 °C for 2–3 h, which was assumed to be sufficient for the CR mixture heat conditioning recommended in practice [6,44]. Due to the expansion of the CR and PET samples post-compaction, a second set of samples were made, where a 13 kPa load was applied on top of the sample post-compaction for 24 h in order to try and reduce the expansion of the samples. The bulk density of the sample was determined geometrically according to EN 12697-29 [45].

The compactability of the asphalt mixture was defined by a version of the Compaction Energy Index [46] adapted by Goh and You [88] to mixtures with high air voids where the index was determined (Fig. 2) by taking the area of the compaction percentage (G_{mm}%) from the 8th gyration to 82% G_{mm} [47]. This was calculated based on the compaction of the water sensitivity samples.

2.2.2. Indirect tensile strength and water sensitivity

The indirect tensile strength (ITS) and water sensitivity were determined according to EN 12697-12 [48] where three samples 99.5 ± 0.5 mm in diameter and 64.0 ± 2.0 mm in height were tested in dry and wet conditions at 25 °C. The wet condition consisted of submerging the sample in water for 70 ± 2 h at 40 °C. The ITS was calculated based on Eq. (1):

$$ITS_{max} = \frac{2P_{max}}{\pi dt} \quad (1)$$

where P is the maximum force to failure, t is the thickness of the sample, and d is the diameter. The indirect tensile strength ratio (ITSR%) was calculated as in Eq. (2).

$$\mathrm{ITSR}\% = 100\% \times \frac{ITS_{wet}}{ITS_{dry}} \quad (2)$$

2.2.3. Fracture energy

The ITS fracture energy was calculated using the area under the stress-strain curve before the maximum stress and after (Fig. 3). The pre-peak area is taken as the fracture energy (FE) and the post-peak area over the peak strain (ε_p) is taken as the post-fracture energy (PE). Their sum is known as the toughness [49,50]. The two mentioned fracture energy methods were also used to evaluate water sensitivity by calculating the FE ratio of the samples as a percentage of dry samples (Eq. (2)), and comparing these results with the ITSR%.

2.2.4. Semi-circular bending

The cracking resistance from PET replacement by volume was measured by the semi-circular bending (SCB) test according to EN 12697-44 [51] (Fig. 4). The cylindrical samples were compacted by gyratory compaction to a height of 50 mm and a diameter of 150 mm, and diamond saw cut on the top and bottom, reducing the height of each sample to 30 ± 3 mm. The samples were cut in half and a notch 10 ± 1 mm deep and 3.5 ± 1 mm wide was cut into the middle of each half. After

Table 3
Asphalt mixture compositions by mass.

Mixture	Control Sandstone %			CR%	PET%	Binder %	Testing
	2/4	0.063/4	Filler			PmB 45/80–65	
Control SDA 4 I	63.1	23.9	7.3	–	–	5.75	Water Sensitivity, Fracture Energy, Surface Texture
CR 2.5%	63.1	21.4	7.3	2.5	–	5.75	
PET 5.1%	63.1	18.9	7.3	–	5.1	5.75	
Control SDA 4 II	62.8	23.8	7.2	–	–	6.10	Cyclic Compression, Semi-Circular Bending
PET 5.1% by Vol.	64.3	19.2	7.4	–	2.8	6.10	

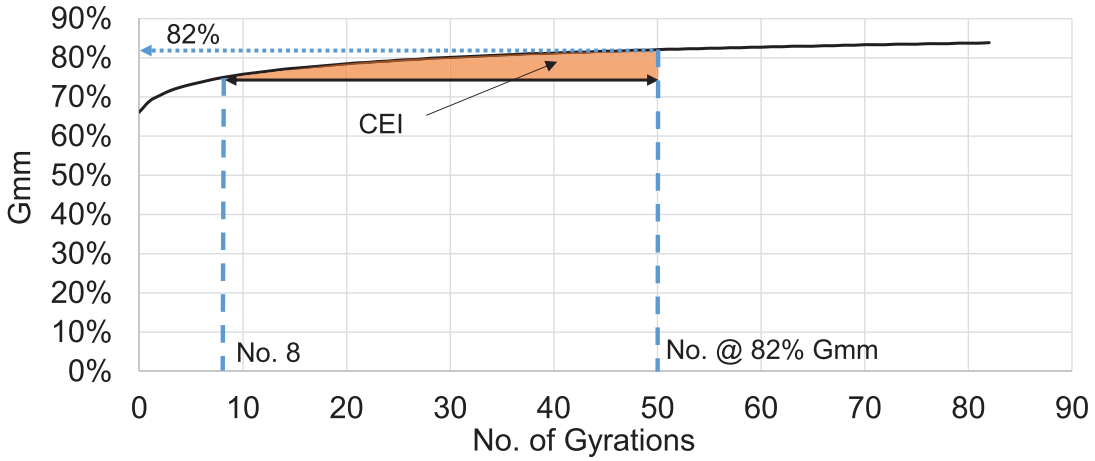

Fig. 2. Modified compaction energy index (CEI %) at 82% G_{mm} based on Goh and You (2012).

conditioning the samples at 0 °C for 4 h, the three point loading was conducted at a vertical deformation rate of 5.0 ± 0.2 mm/min. From this, the fracture Toughness, K_{Ic} ($N/m^{3/2}$), was calculated from the peak-stress σ_{max}, as in Eq. (3),

$$\sigma_{max} = \frac{4.263\, F_{max}}{D \times t} \tag{3}$$

where F_{max} is the peak load, D is the diameter of the specimen and t is the thickness. This can be used to compute Eq. (4) as follows:

$$K_{Ic} = \sigma_{max} f\left(\frac{a}{W}\right) \tag{4}$$

where $f\left(\frac{a}{W}\right)$ is a parameter incorporating the specimen height (W) and notch depth (a).

2.2.5. Cyclic compression

The resistance to intermediate temperature deformation of the control and optimized PET mixtures were characterized by the cyclic compression test, based on the German standard [53], which is a more

Fig. 4. Semi-circular bending (SCB) testing (left) after conditioning at 0 °C (EN 12697-44) and cyclic compression test setup [52] (right).

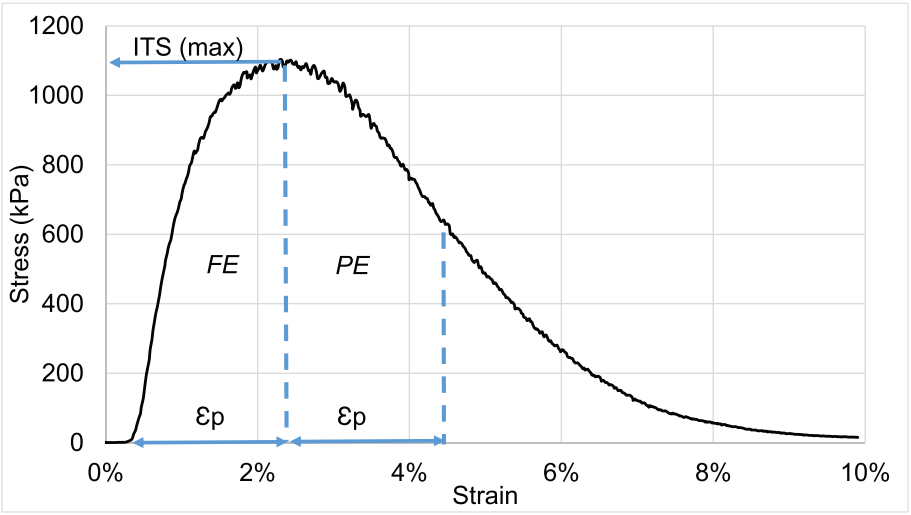

Fig. 3. Fracture energy method applied to ITS stress-strain curve based on Park et al., 2015.

explicit version of the European standard [54]. The asphalt mixture is compacted to cylinders 100 ± 1 mm in diameter and 60 ± 1 mm in height, with graphite applied to the top and bottom surface to encourage more homogenous contact with the loading plate. The samples were conditioned at 50 °C before the test for 4 h and the sample was loaded axially for 1.7 s cycles and 1.5 s rest periods (Fig. 4). The upper and lower stresses were set at 0.350 and 0.025 MPa, respectively. The loading proceeded until the cumulative axial strain, ε_n had reached 40% (Eq. (5)):

$$\varepsilon_n = \frac{(h_0 - h_n)}{h_0} \text{ x } 1000 \quad (5)$$

where h_0 is the specimen height after initial loading, h_n is the specimen height after n cycles of loading. Three stages can be distinguished.

2.2.6. Sound absorption

The sound absorption coefficients of the mixtures were measured using a Brüel & Kjær impedance tube model 4206. The measurements were carried out according to the transfer function method described in ISO 10534-2 (Fig. 5). The cylindrical samples with 100 mm diameters were sealed in the tube in two stages. First, the curved surface of the sample was covered with a stiff adhesive tape. This was done in order to seal the gap between the samples and the inner curved surface of the impedance tube to avoid acoustic energy leakage and unwanted vibration. For this purpose the samples were abraded using a sandpaper machine so that a tolerance of −0.2 mm was created to create enough gap size for the sealing tape. Second, the rim of the sample was sealed using a petroleum jelly as recommended in ISO 10534-2. This would help avoid acoustic energy leakage through the cracks around the rim of the sample. Tests were carried out three times for each sample, with a rotation of 120° at each step, to count for possible randomness of the surface texture. The results were then averaged to calculate the absorption coefficient of each mixture.

2.2.7. Texture scanning

The surface texture of the asphalt mixture samples was measured with an Ames Engineering 9400HD 3D laser scanner (Fig. 6). The tests were conduction on 6 cylindrical asphalt samples with a diameter of 100 mm (see Section 2.2.1) of each type. The test was conducted by placing the sample horizontally under the device and conducting a 50 × 50 mm area scan. The resolutions were 0.005 mm vertically, 0.006 mm along the length of the scan and 0.025 mm for the width. Each area scan consisted of 200 scan lines and was used to calculate the average mean profile depth (MPD), skewness (R_{sk}), kurtosis (R_{ku}) and length/ area ratio via the Ames software. The MPD, where represents the texture amplitude in a single value, was calculated removing wavelengths below 2.5 mm as prescribed by ISO 13473-1, however,

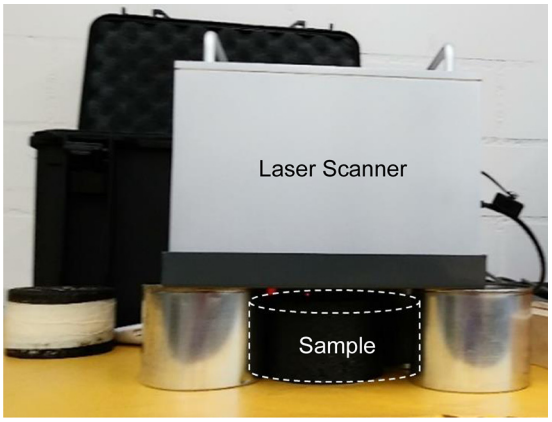

Fig. 6. Scanning asphalt texture with Ames Engineering 9400HD 3D laser scanner.

the maximum scan line was limited to 50 mm due to the size of the samples, less than the 100 mm minimum prescribed. The skewness is a measure of how positive or negative the texture is, with negative texture (<0) meaning less vibration and potentially less noise [41]. Finally, kurtosis is a measure of the spikiness/ bumpiness of the surface, with more bumpiness at values of less than 3 [55]. This can be an indication of the wearing behavior.

Furthermore, 200 of the scan lines were used to calculate the texture level ($L_{TX,\lambda}$) relative to the texture wavelengths, λ, by taking the 1/3rd octave band power spectral density graphs for each scanline and using Eq. (6) derived from ISO 13473-4.

$$L_{TX,\lambda} = 10 \log \left(\frac{Z_{p,\lambda} * 0.232f}{{a_{ref}}^2} \right) dB \quad (6)$$

where $Z_{p,\lambda}$ is the 1/3rd octave band power spectral density (PSD) amplitude for a certain texture bandwidth, λ, *0.232f* is the bandwidth of the 1/3rd octave band (with spatial center frequency $f = 1/\lambda$, and a_{ref} is the reference value of the surface profile amplitude (10^{-6} m given by ISO 13473-4). Given the sample sizes and the resolution of the scanner, L_{TX} was analyzed for texture wavelengths of 0.05–50 mm. ISO 13473-4 advises that the maximum texture wavelength analyzed, λ_{max} be much smaller than the analysis length, *l*, whereas in our case, $\lambda_{max} = l$. Given that ISO 13473-4 is written for laser scanners pulled by a car driving on the road, maximum wavelengths of greater than 50 mm are more feasible than with laboratory samples. However, the modified laboratory method employed here is more precise than the field method prescribed as it is standstill and not attached to a moving vehicle.

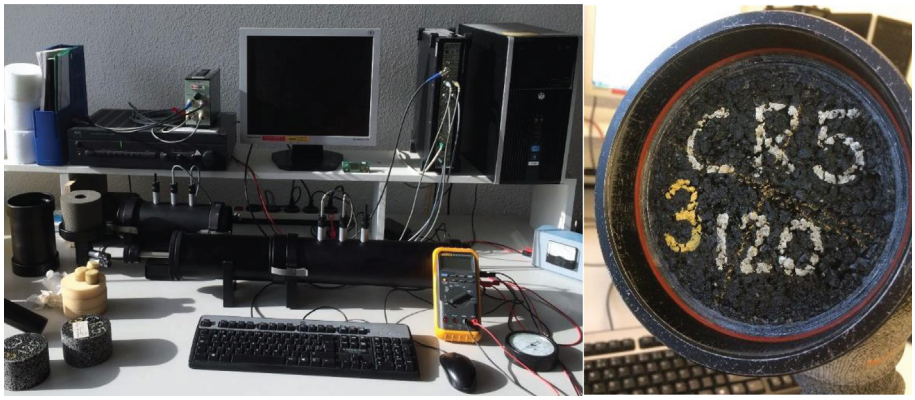

Fig. 5. Sound absorption measurement setup with 100 mm cylindrical sample.

3. Results and discussion

3.1. Volumetrics and compaction

The volumetric properties of the asphalt mixtures are shown in Table 4. Firstly, it can be noted that the maximum density of the samples is lower with the lighter waste aggregates. While the samples were initially compacted to be as close to 64 mm in height as possible, the first set of CR and PET samples with replacement by mass tended to expand after the compaction during the cooling phase of the sample preparation. This was around 2 mm (3.1%) for the CR and 4.8 mm (7.5%) for PET, which was not present in the control and corresponded to the relative replacement rates of CR and PET. This expansion resulted in a voids content of 18% and 21.9% for the CR and PET mixtures, respectively, meaning that these samples were in the porous asphalt range that is defined as around 20% and up [41]. To hinder the expansion, a second set of CR and PET samples had a 13 kPa load placed on top during cooling where the asphalt is most likely to move, while the samples are left with in the mould for 24 h. After the cooling, the expansion is thought to be less likely. This significantly reduced the expansion of the CR mixture to 0.9 mm (1.4%), while having little effect on the PET mixture which had an expansion of 3.9 mm (6.1%). Based on the air voids, the second set of PET samples were discarded, while the two sets of CR samples are herein referred to as "CR 2.5% post load" for the samples with pressure applied in the 24 h after compaction.

The differences in the post compaction expansion in loading can be understood by looking at the compaction energy and number of gyrations to reach 83% Gmm shown in Fig. 7. The PET samples were much more difficult to compact than the control, while the CR samples, agreeing with previous studies [56], were relatively easy to compact. This is due to on one hand, the CR being much softer than the PET, but also due to the higher content of the latter, and being more flaky, which has been reported to decrease the compactability [57].

Given that a certain conditioning time with already allowed for swelling [58] in the case of CR, the expansion is speculated to be due to the hyperelasticity of the CR [59], where the expansion is a response to the shear forces from the gyratory compaction [60,61]. For this reason, adding a load is recommended by some researchers [56]. While this effect is said to be specific to laboratory compaction, some field guidelines dictate the screening out of CR particles of above 2 mm for this reason [62], which is indicative of this being an issue in the field as well.

For the PET, due to the force of compaction required, elastic compression of the PET in the mixture may be a factor, which would recover when the samples is demolded. The long shape of the PET is also a factor in the PET adding more stiffness to the mixture [35]. Hence, these effects were more difficult to mitigate with the post compaction load than with CR. Due to the much smaller amount of research on PET, this effect has not been reported or discussed. Otherwise, it is clear that higher PET replacement of fine aggregates needs to be done on a volume basis to ensure adequate compactability and volumetric properties.

Table 4
Volumetric properties of asphalt mixtures for ITSR%.

Sample	% Δh[a]	Bulk Density (kg/m^3) EN 12697-29	Max. Density (kg/m^3) EN 12697-5	Air Voids %	VMA % 8	VFA %
Control SDA 4 I	–	2061.9	2463.3	16.3	27.1	39.8
Std Dev	–	*9.2*	*20.9*	*0.4*	*0.3*	*0.7*
CR 2.5%	3.2	1964.0	2395.6	18.0	28.2	36.2
Std Dev	*0.4*	*7.1*	*10.1*	*0.3*	*0.3*	*0.5*
CR 2.5% post load[b]	1.4	1987.4	2395.6	17.0	27.4	37.8
Std Dev	*0.2*	*4.0*	*10.1*	*0.2*	*0.1*	*0.3*
PET 5.1%	6.1	1845.4	2363.0	21.9	31.4	30.3
Std Dev	*0.9*	*28.4*	*15.8*	*1.2*	*1.1*	*1.5*
PET 5.1% post load[b]	4.5	1857.9	2363.0	21.4	30.9	30.9
Std Dev	*0.1*	*3.3*	*15.8*	*0.1*	*0.1*	*0.2*

[a] Difference in sample height between after compaction and after 24 h at room temperature.
[b] 13 kPa load applied post-compaction for same mixture.

3.2. Indirect tensile strength and water sensitivity

The ITS and water sensitivity results are shown in Table 5. In terms of ITS in general, the values for CR and PET samples are significantly lower relative to the control. This is due to both the higher air voids content and the CR and PET aggregates being softer than sandstone. In the case of CR mixtures, the amount of CR used is significantly higher than the conventionally used amounts of 1% [ref]. In case of PET mixtures, the smoother surface of the PET particles would naturally have lower adhesion to bitumen. In terms of the ITSR%, the PET samples perform somewhat worse than the control, but this is still above the national requirement of 70% (SN 640 431-1c-NA) [63] and in agreement with previous testing of PET mixtures [34,35,39,64]. The CR samples on the other hand, despite having a lower ITS, have a significantly lower ITSR%. This is in agreement with previous studies of untreated CR added with the dry process. This has been attributed to the CR particles negatively affecting the adhesion of the aggregates and binder [11,14]. The source of this is likely due to some surface energy incompatibility with the bitumen, which is why many CRs are surface treated before being added to asphalt [65]. The 2.5% replacement rate can also be considered especially high compared to what is typically tested.

The PET, which was also replaced at a higher quantity than the CR is more adequate as an aggregate. Previous studies on PET incorporation found that the moisture resistance can be improved [32,66], but with PET contents much lower than 5.1% by mass of the aggregates. Where PET contents were closer to those of the current study, the moisture resistance was also found to be lower [34,35,67,68].

3.3. Indirect tensile strength fracture energy

3.3.1. Dry samples

While the ITS is based on the maximum load, the fracture energy is calculated from the stress-strain diagram. For the fracture energy (FE) shown in Fig. 8, which is an indicator of cracking resistance prior to the peak load, the CR samples required much less energy to fail. The PET samples on the other hand perform much better; achieving 85% of the control for the FE in comparison to 70% for the ITS (Table 5). The post-fracture energy (PE), an indication of crack propagation, shows a similar pattern to the FE.

3.3.2. Water sensitivity based on fracture energy

The water sensitivity can also be looked at with fracture energy. As expected, the fracture energy as well as the post fracture energy in wet state are less than dry state for all samples, indicating less energy is required for sample to fail. However, in the case of the FE and PE, the effects of water are not as significant as with ITSR% (Fig. 8) as the behavior of the material during the entirety of the test is considered. For the control and PET samples, they show considerably less reduction after water conditioning, the results showing that the wet samples retained 90–100% of their energy absorption during indirect tensile loading. This is due to the fact that classic ITSR% considers only the peak load, and thus, favoring stiffer mixtures over more ductile ones. The CR samples degraded significantly more as previously indicated.

3.4. Sound absorption

Fig. 9 shows the absorption coefficient for the samples versus the control SDA 4, along the frequency range of 400 Hz to 1200 Hz on

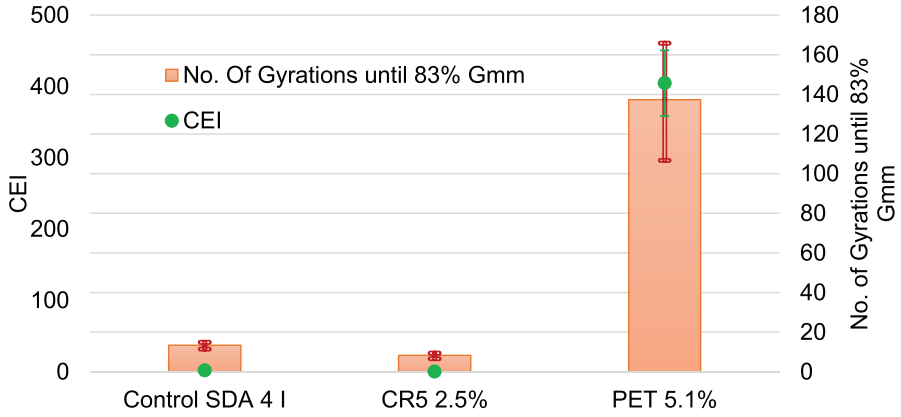

Fig. 7. Number of gyrations to 83% of maximum density and CEI of ITS% gyratory samples.

Table 5
ITS and water sensitivity results.

Sample	Max Load Dry (kPa)	Max Load Wet (kPa)	ITSR %
Control SDA 4 I	1127.3	915.0	81.2
Std Dev	*43.9*	*15.7*	
CR 2.5%	511.8	294.6	57.6
Std Dev	*19.6*	*17.6*	
CR 2.5% post load	596.5	326.2	54.7
Std Dev	9.5	21.1	
PET 5.1%	797.8	580.8	72.8
Std Dev	*57.2*	*44.6*	

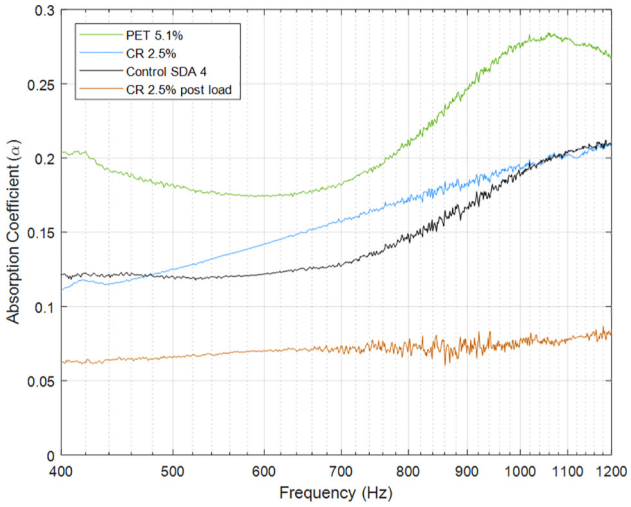

Fig. 9. Sound absorption of gyratory compacted samples for ITS.

semi-logarithmic axes. This frequency range is selected since this is the range where traffic noise is dominant, i.e. effective noise reduction due to absorption is expected in this range. The absorption coefficients of the crumb rubber mixture (18% air voids), the crumb rubber post load mixture (17% air void), the PET mixture (21.9% air voids) and control mixture (16.3% air voids) reach a maximum of 0.21, 0.09, 0.28 and 0.21 respectively. In general, these values of absorption coefficient are not considered significant.

Although some studies show higher values for the absorption coefficients of different asphalt mixtures, the measurements in the current study do not show absorption coefficient values which would indicate significant sound absorption. This might be due to several factors: (1) The difference between the measurement methods i.e. in situ or reverberation chamber measurements instead of normal incidence impedance tube method used in the current study, (2) the difference between the air void percentage, e.g. 20–30% air void content in some studies [15,69–74] compared to 16%–22% in this study, and (3) the difference in the precision of the sealing practice of the samples. The studies with similar air voids to ones studied here also had similar

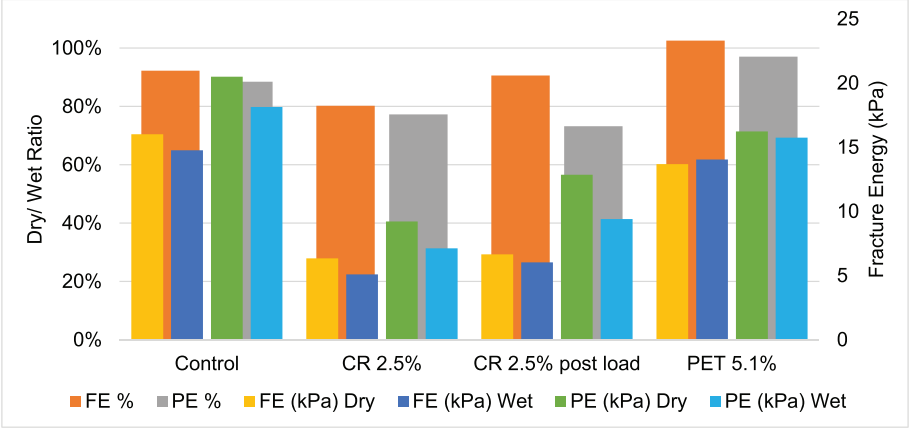

Fig. 8. Indirect tensile fracture energy (FE) and post-fracture energy (PE) before and after water conditioning.

Table 6
Texture parameters of gyratory compacted samples.

Mixture	Air Voids %	MPD (mm)	R_{sk} (mm)	R_{ku} (mm)
Control SDA 4I	16.3	0.727	−1.378	2.234
Std Dev	*0.4*	*0.047*	*0.049*	*0.290*
CR 2.5%	18.0	0.507	−1.572	3.279
Std Dev	*0.3*	*0.028*	*0.064*	*0.290*
CR 2.5% post load	17.0	0.447	−1.726	3.990
Std Dev	*0.2*	*0.034*	*0.132*	*0.651*
PET 5.1%	21.9	0.752	−1.322	2.357
Std Dev	*1.2*	*0.033*	*0.028*	*0.210*

absorption coefficients [75,76], indicating that SDA might not be porous enough as a sound reduction surface compared to porous asphalt as also found in the literature [41]. This is to be further investigated in future work.

3.5. Surface texture

The surface texture parameters are show in Table 6. The Mean Profile Depth (MPD), an indication of noise properties, was found to be significantly lower in the CR samples and only somewhat higher than the control for the PET samples. The decrease MPD was also reported in previous studies with dry process CR incorporation into asphalt [13,77,78]. This has been correlated to a reduction in the tire/pavement noise generation for porous mixtures [79].

The texture skewness (R_{sk}) is a parameter where a negative value [80] indicates a profile less susceptible to generating noise from vibrations. While all of the mixtures show negative textures, the CR mixtures are more negative than the control and PET sample. Kurtosis (R_{ku}) is an indication of the bumpiness/ jaggedness of the surface, with a more bumpy surface (<3) being less susceptible to wear [55]. The CR mixtures are significantly higher in this, possibly indicating that they could be more susceptible to wearing, while the PET mixture is very similar to the control. Similar results were found previously for CR mixtures, although also with a high standard deviation as in the present study [81] meaning that the results should be interpreted cautiously.

The texture level (L_{tx}) of the pavements in the wavelength range 0.1 to 100 mm is shown in Fig. 10. As found with the MPD, in comparison to the control mixture the texture level is much lower for the CR samples and similar with the PET. This is true for both the macro (50–16 mm) and microtexture (<8 mm). This trend has been observed previously with dry CR incorporated for gap-graded mixtures [82,83]. This leve1 is slightly lower for the CR sample with lower air voids, while the PET sample performs the same as the control despite having an air voids content that is 6% higher. The findings indicate a bias of the texture level to the material over the air void content.

A lower texture amplitude at wavelengths 2–8 mm has been correlated to higher noise generation at higher frequencies (200–5000 Hz), while lower amplitude at 16–160 mm has been correlated to lower noise at lower frequencies below 800 Hz [82,84,85], so there may be a reduction in low frequency noise but an increase for higher frequencies. This can been explained by the higher texture level / lower frequency noise corresponding to tire vibrations and the lower texture higher frequency noise corresponding to aerodynamic effects of the air travelling through the pavement [82]. The CR incorporation may be favorable to dampening the tire-vibration effects. The lower macrotexture may also reduce the fuel consumption for vehicles [86]. Lower texture also indicates lower skid resistance [87] and lower safety, which should also be considered.

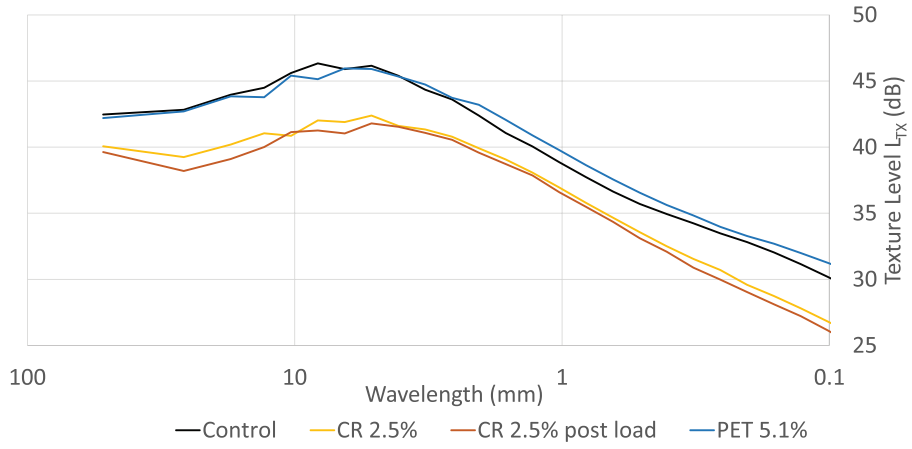

Fig. 10. Texture levels (L_{tx}) of gyratory compacted samples.

Table 7
Volumetric properties of SCB test samples.

Sample	% Δh[a]	Bulk Density (kg/m^3) EN 12697-29	Max. Density (kg/m^3) EN 12697-5	Air Voids %	VMA %	VFA %
Control SDA 4 II	–	2061.9	2463.3	16.3	27.1	39.8
Std Dev	–	*9.2*	*20.9*	*0.4*	*0.3*	*0.7*
PET 5.1% by vol[b]	0.4	1968.1	2404.6	18.2	28.7	36.8
Std Dev	*0.6*	*7.5*	*2.0*	*0.3*	*0.3*	*0.5*

[a] Difference in sample height between after compaction and after 24 h at room temperature.
[b] PET replaced by volume instead of mass.

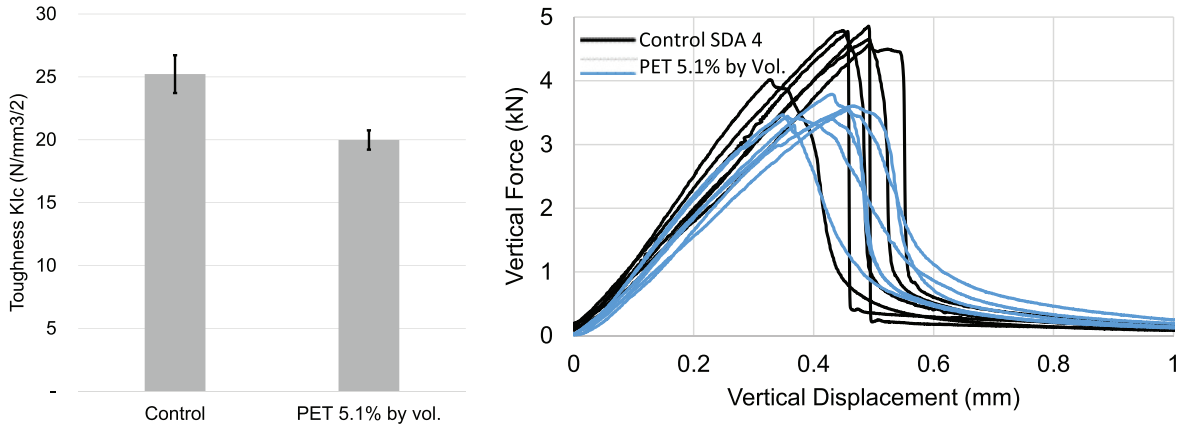

Fig. 11. Semi-circular bending (SCB) toughness (left) and loading curves (right) at 0 °C.

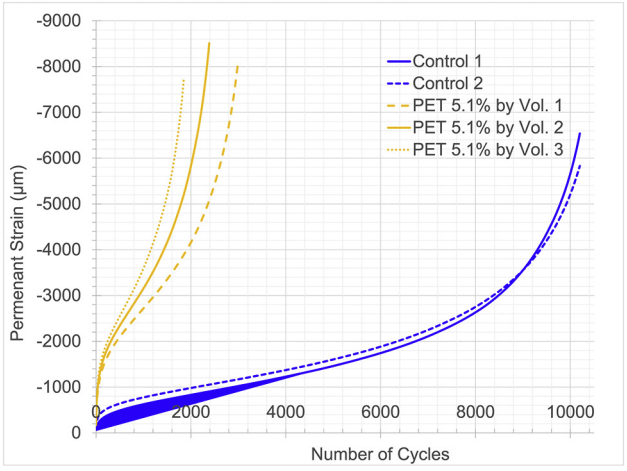

Fig. 12. Cyclic compression test results for each sample at 50 °C.

3.6. Performance of optimized asphalt mixtures with PET replacement by volume

The results from the replacement of aggregate sand by CR and PET (Table 7) showed that while the CR replacement had very low ITS and high water sensitivity, the PET samples showed interesting results with regards to acceptable water sensitivity and ITS fracture energy similar to that of the control. However, the compaction of the PET mixture was very difficult, and resulted in an air void content in the porous asphalt range. To mitigate this, replacing the 5.1% PET by volume (2.8% by mass) was made and compared with the control mixture.

The volumetric properties are shown in Table 7. The samples were again compacted to 16% air voids, but experienced the same elastic rebound, although at a less significant rate of 0.4% as opposed to the previous values at over 6% when the PET was replaced by mass. The compaction was also a challenge, with the samples only compacted to an average of 18.2% voids due to the length of time it took for compaction. However, the 100 mm cyclic compression samples did not have such issues, so the compaction very well could be an outlier related to comparing the 150 mm diameter samples with the 100 mm samples, with the former taking many more cycles to compact.

The cracking susceptibility at 0 °C using the SCB results (Fig. 11) show that the PET sample had a lower cracking resistance at 0 °C, around 80% of the control sample result. These results diverge from the results of ITS in Table 5, where the fracture energy was similar to the control for the PET mixture. However the strength using ITS was 70.8% and 63.5% of control for dry and wet samples respectively. This could be explained by the lower temperature (0 °C) used for SCB test compared to ITS at (25 °C). However, it is also worth noting that the loading curves were less sharp after the peak than for the control, indicating a less brittle post fracture failure.

The cyclic compression results at 50 °C are shown in Fig. 12. Here, the PET samples are able to resist far fewer cycles than the control at higher temperatures, similar to other studies with higher PET contents [35]. While one issue is the higher voids content in the PET samples, when considering the previous SCB cracking results, there is likely a reduction in the internal cohesion from the PET replacement, most likely from a reduction in adhesion of this material compared to the virgin aggregates. Furthermore the effect of the binder and its softening at higher temperatures should be considered. At higher temperatures the binder becomes soft and the effect of sand more prominent. This suggests that replacing sand with PET waste should be further optimized considering the type and amount of base binder as well as amount of waste PET. Comparing the low temperature results in the SCB test (Fig. 11) and the high temperature behavior in CCT, it is apparent that temperature plays an important role for PET modified mixtures. While at low temperatures the three component composite bitumen/aggregate/PET behave more elastic at high temperature close to the softening point of bitumen on of these component i.e. bitumen and to a certain extent PET starts to become softer which has a direct effect on the permanent deformation shown in Fig. 12.

4. Conclusions

The current study presented the partial replacement of Semi-Dense Asphalt (SDA) sand fraction by waste Crumb Rubber (CR) and waste Polyethylene Terephthalate (PET). The conclusions from the study are as follows:

- Sand replacement by elastic aggregates like CR and PET can result in elastic rebound post-compaction. While this can be somewhat mitigated in the lab, it could occur in the field when these type of materials, including other plastics, are added to asphalt aggregates in the field. It needs to be accounted in the pavement placement and quality control. This can be done by accounting for the expansion in the road design or modifying the aggregates structure. Not doing so can results in higher than planned air void contents, and subsequent issues with pavement durability.
- CR replacement of sand in SDA significantly reduces the ITS and ITSR% of the mixtures, making it a poor replacement for sand.
- The surface texture is improved from CR replacement in terms of fuel consumption, and possibly the noise reduction properties.

- The sound absorption seems to be affected mostly by the air void content and not the sand replacement, but remains fairly modest for SDA and the PET replacement mixture with higher air voids.
- The PET replacement of sand in SDA by mass reduces the ITS of the mixtures while being similar in fracture energy, making the mixture more ductile. However, this mixture is very difficult to compact.
- PET replacement of sand in SDA by volume results in a reduction of low temperature cracking and permanent deformation resistance at higher temperatures. However the performance at higher temperatures diverges more significantly from the reference.
- The effect of temperature and difference in the behavior of the three component composite has to be considered in the design of such mixtures.

While finding opportunities for replacement in asphalt mixtures is important, it is not recommended to directly replace significant fractions of sand in porous mixtures like SDA with CR and PET. This can lead to poor cracking resistance, moisture sensitivity and rutting resistance. When these materials are used in asphalt mixtures with higher than conventional porosities, they should be used more as modifiers for the bitumen or additives in mixtures, as is already the case with CR. Further considerations are optimization of base binder type and content, waste content, hot asphalt odor modification and waste pretreatment solutions.

CRediT authorship contribution statement

Peter Mikhailenko: Conceptualization, Methodology, Investigation, Visualization, Writing - original draft, Writing - review & editing. **Zhengyin Piao**: Investigation, Writing - review & editing. **Muhammad Rafiq Kakar**: Investigation, Methodology, Writing - review & editing. **Sahand Athari**: Investigation, Writing - original draft. **Moises Bueno**: Conceptualization, Writing - review & editing. **Lily D. Poulikakos**: Conceptualization, Writing - review & editing, Project administration, Funding acquisition.

Declaration of Competing Interest

The authors declare that they have no known competing financial interests or personal relationships that could have appeared to influence the work reported in this paper.

Acknowledgements

The current project is part of the Swiss National Science Foundation (SNF) grant 205121_178991/1 for the project titled “Urban Mining for Low Noise Urban Roads and Optimized Design of Street Canyons”. The authors would like to acknowledge the contributions of the Empa Concrete and Asphalt lab for assistance with the testing, notably Roland Takacs, Markus Erb, Hans Kienast, Freddy Bürki and Simon Küntzel. Additional thanks goes to Kurt Heutschi and Reto Pieren of the Acoustics/Noise Control at Empa for his help with reviewing the paper.

References

[1] R. Siddique, G. Singh, M. Singh, Recycle option for metallurgical by-product (spent foundry sand) in green concrete for sustainable construction, J. Clean. Prod. 172 (2018) 1111–1120, https://doi.org/10.1016/j.jclepro.2017.10.255.

[2] L.D. Poulikakos, C. Papadaskalopoulou, B. Hofko, F. Gschösser, A. Cannone Falchetto, M. Bueno, M. Arraigada, J. Sousa, R. Ruiz, C. Petit, M. Loizidou, M.N. Partl, Harvesting the unexplored potential of European waste materials for road construction, Resour. Conserv. Recycl. 116 (2017) 32–44, https://doi.org/10.1016/j.resconrec.2016.09.008.

[3] Z. Piao, P. Mikhailenko, M.R. Kakar, M. Bueno, S. Hellweg, L.D. Poulikakos, Urban mining for asphalt pavements: a review, J. Clean. Prod. 280 (2021) 124916, https://doi.org/10.1016/j.jclepro.2020.124916.

[4] N.S. Mashaan, A.H. Ali, M.R. Karim, M. Abdelaziz, A review on using crumb rubber in reinforcement of asphalt pavement, Sci. World J. 2014 (2014) https://doi.org/10.1155/2014/214612.

[5] Z. Piao, M. Bueno, P. Mikhailenko, M.R. Kakar, D. Biondini, L. Poulikakos, S. Hellweg, Life cycle assessment of asphalt pavements using crumb rubber: a comparative analysis, RILEM Int. Symp. Bitum. Mater. - ISBM Lyon 2020, Lyon, France, 2020.

[6] I. Rodríguez-Fernández, M.C. Cavalli, L. Poulikakos, M. Bueno, Recyclability of asphalt mixtures with crumb rubber incorporated by dry process: a laboratory investigation, Materials 13 (2020) 2870, https://doi.org/10.3390/ma13122870.

[7] C. Loderer, M.N. Partl, L.D. Poulikakos, Effect of crumb rubber production technology on performance of modified bitumen, Constr. Build. Mater. 191 (2018) 1159–1171, https://doi.org/10.1016/j.conbuildmat.2018.10.046.

[8] N. Tang, R. Dong, Anti-aging potential of sulphur in terminal blend rubberized asphalt binder, Constr. Build. Mater. 250 (2020) 118858, https://doi.org/10.1016/j.conbuildmat.2020.118858.

[9] P. Lastra-González, M.A. Calzada-Pérez, D. Castro-Fresno, Á. Vega-Zamanillo, I. Indacoechea-Vega, Comparative analysis of the performance of asphalt concretes modified by dry way with polymeric waste, Constr. Build. Mater. 112 (2016) 1133–1140, https://doi.org/10.1016/j.conbuildmat.2016.02.156.

[10] F. Moreno-Navarro, M.C. Rubio-Gámez, A.J.D. Barco-Carrión, Tire crumb rubber effect on hot bituminous mixtures fatigue-cracking behaviour, J. Civ. Eng. Manag. 22 (2016) 65–72, https://doi.org/10.3846/13923730.2014.897982.

[11] F. Moreno-Navarro, M. Sol-Sánchez, M.C. Rubio-Gámez, M. Segarra-Martínez, The use of additives for the improvement of the mechanical behavior of high modulus asphalt mixes, Constr. Build. Mater. 70 (2014) 65–70, https://doi.org/10.1016/j.conbuildmat.2014.07.115.

[12] W. Cao, Study on properties of recycled tire rubber modified asphalt mixtures using dry process, Constr. Build. Mater. 21 (2007) 1011–1015, https://doi.org/10.1016/j.conbuildmat.2006.02.004.

[13] S. Eskandarsefat, C. Sangiorgi, G. Dondi, R. Lamperti, Recycling asphalt pavement and tire rubber: a full laboratory and field scale study, Constr. Build. Mater. 176 (2018) 283–294, https://doi.org/10.1016/j.conbuildmat.2018.05.031.

[14] A. Cetin, Effects of crumb rubber size and concentration on performance of porous asphalt mixtures, Int. J. Polym. Sci. 2013 (2013) 1–10, https://doi.org/10.1155/2013/789612.

[15] M. Liu, X. Huang, G. Xue, Effects of double layer porous asphalt pavement of urban streets on noise reduction, Int. J. Sustain. Built Environ. 5 (2016) 183–196, https://doi.org/10.1016/j.ijsbe.2016.02.001.

[16] S.E. Paje, M. Bueno, U. Viñuela, F. Terán, Toward the acoustical characterization of asphalt pavements: analysis of the tire/road sound from a porous surface, J. Acoust. Soc. Am. 125 (2009) 5–7, https://doi.org/10.1121/1.3025911.

[17] L.M. Pierce, J.P. Mahoney, S. Muench, H.J. Munden, M. Waters, J. Uhlmeyer, Quieter hot-mix asphalt pavements in Washington state, Transp. Res. Rec. 2095 (2009) 84–92, https://doi.org/10.3141/2095-09.

[18] A.F. Ahmad, A.R. Razali, I.S.M. Razelan, Utilization of polyethylene terephthalate (PET) in asphalt pavement: a review, IOP Conf. Ser. Mater. Sci. Eng. 203 (2017), 012004, https://doi.org/10.1088/1757-899X/203/1/012004.

[19] Keystone-SDA/sb, Plastic bottle recycling gets easier in Switzerland, SWI Swissinfoch, https://www.swissinfo.ch/eng/recycling_plastic-bottle-recycling-gets-easier-in-switzerland-/45477432 2020 (accessed November 13, 2020).

[20] R. Zhang, X. Ma, X. Shen, Y. Zhai, T. Zhang, C. Ji, J. Hong, PET bottles recycling in China: an LCA coupled with LCC case study of blanket production made of waste PET bottles, J. Environ. Manag. 260 (2020) 110062, https://doi.org/10.1016/j.jenvman.2019.110062.

[21] M. Alzuhairi, A. Al-Ghaban, S. Almutalabi, Chemical recycling of polyethylene terephthalate (waste water bottles) for improving the properties of asphalt mixture, MATEC Web Conf. 162 (2018), 01042, https://doi.org/10.1051/matecconf/201816201042.

[22] Z. Leng, A. Sreeram, R.K. Padhan, Z. Tan, Value-added application of waste PET based additives in bituminous mixtures containing high percentage of reclaimed asphalt pavement (RAP), J. Clean. Prod. 196 (2018) 615–625, https://doi.org/10.1016/j.jclepro.2018.06.119.

[23] C. Maharaj, R. Maharaj, J. Maynard, The effect of polyethylene terephthalate particle size and concentration on the properties of asphalt and bitumen as an additive, Prog. Rubber Plast. Recycl. Technol. 31 (2015) 1–23, https://doi.org/10.1177/147776061503100101.

[24] M. Ameri, D. Nasr, Performance properties of devulcanized waste PET modified asphalt mixtures, Pet. Sci. Technol. 35 (2017) 99–104, https://doi.org/10.1080/10916466.2016.1251457.

[25] D.R. Merkel, W. Kuang, D. Malhotra, G. Petrossian, L. Zhong, K.L. Simmons, J. Zhang, L. Cosimbescu, Waste PET chemical processing to terephthalic amides and their effect on asphalt performance, ACS Sustain. Chem. Eng. 8 (2020) 5615–5625, https://doi.org/10.1021/acssuschemeng.0c00036.

[26] A.M. Mosa, I.T. Jawad, L.A. Salem, Modification of the properties of warm mix asphalt using recycled plastic bottles, Int. J. Eng. 31 (2018) 1514–1520, https://doi.org/10.5829/ije.2018.31.09c.06.

[27] O.M. Ogundipe, The use of polyethylene terephthalate waste for modifying asphalt concrete using the Marshall test, Slovak J. Civ. Eng. 27 (2019) 9–15, https://doi.org/10.2478/sjce-2019-0010.

[28] J. Paben, How a company is turning PET into durable asphalt, Plast. Recycl. Update, 2020 https://resource-recycling.com/plastics/2020/08/19/how-a-company-is-turning-pet-into-durable-asphalt/ , (accessed March 22, 2021).

[29] T. Baghaee Moghaddam, M.R. Karim, T. Syammaun, Dynamic properties of stone mastic asphalt mixtures containing waste plastic bottles, Constr. Build. Mater. 34 (2012) 236–242, https://doi.org/10.1016/j.conbuildmat.2012.02.054.

[30] Z. Dehghan, A. Modarres, Evaluating the fatigue properties of hot mix asphalt reinforced by recycled PET fibers using 4-point bending test, Constr. Build. Mater. 139 (2017) 384–393, https://doi.org/10.1016/j.conbuildmat.2017.02.082.
[31] A. Modarres, H. Hamedi, Effect of waste plastic bottles on the stiffness and fatigue properties of modified asphalt mixes, Mater. Des. 61 (2014) 8–15, https://doi.org/10.1016/j.matdes.2014.04.046.
[32] M.A.H. Al-Jumaili, Sustainability of asphalt paving materials containing different waste materials, IOP Conf. Ser. Mater. Sci. Eng. 454 (2018), 012176, https://doi.org/10.1088/1757-899X/454/1/012176.
[33] T. Baghaee Moghaddam, M. Soltani, M.R. Karim, Evaluation of permanent deformation characteristics of unmodified and polyethylene terephthalate modified asphalt mixtures using dynamic creep test, Mater. Des. 53 (2014) 317–324, https://doi.org/10.1016/j.matdes.2013.07.015.
[34] E. Ahmadinia, M. Zargar, M.R. Karim, M. Abdelaziz, E. Ahmadinia, Performance evaluation of utilization of waste polyethylene terephthalate (PET) in stone mastic asphalt, Constr. Build. Mater. 36 (2012) 984–989, https://doi.org/10.1016/j.conbuildmat.2012.06.015.
[35] H. Taherkhani, M.R. Arshadi, Investigating the mechanical properties of asphalt concrete containing waste polyethylene terephthalate, Road Mater. Pavement Des. 20 (2019) 381–398, https://doi.org/10.1080/14680629.2017.1395354.
[36] M.A. Dalhat, H.I. Al-Abdul Wahhab, K. Al-Adham, Recycled plastic waste asphalt concrete via mineral aggregate substitution and binder modification, J. Mater. Civ. Eng. 31 (2019), 04019134, https://doi.org/10.1061/(ASCE)MT.1943-5533.0002744.
[37] A. Hassani, H. Ganjidoust, A.A. Maghanaki, Use of plastic waste (poly-ethylene terephthalate) in asphalt concrete mixture as aggregate replacement, Waste Manag. Res. 23 (2005) 322–327, https://doi.org/10.1177/0734242X05056739.
[38] W.M.N.W.A. Rahman, A.F.A. Wahab, Green pavement using recycled polyethylene terephthalate (PET) as partial fine aggregate replacement in modified asphalt, Procedia Eng. 53 (2013) 124–128, https://doi.org/10.1016/j.proeng.2013.02.018.
[39] A.S. Esfandabad, S.M. Motevalizadeh, R. Sedghi, P. Ayar, S.M. Asgharzadeh, Fracture and mechanical properties of asphalt mixtures containing granular polyethylene terephthalate (PET), Constr. Build. Mater. 259 (2020) 120410, https://doi.org/10.1016/j.conbuildmat.2020.120410.
[40] EN 1426, Bitumen and Bituminous Binders. Determination of Needle Penetration, 2015.
[41] P. Mikhailenko, Z. Piao, M.R. Kakar, M. Bueno, S. Athari, R. Pieren, K. Heutschi, L. Poulikakos, Low-noise pavement technologies and evaluation techniques: a literature review, Int. J. Pavement Eng. (2020) https://doi.org/10.1080/10298436.2020.1830091.
[42] S.N. Swiss Standard, 640 436 Semidichtes Mischgut und Deckschichten Festlegungen, Anforderungen, Konzeption und Ausführung, 2013.
[43] Z. Sun, C. Wang, X. Hao, W. Li, X. Zhang, Quantitative evaluation for shape characteristics of aggregate particles based on 3D point cloud data, Constr. Build. Mater. 263 (2020) 120156, https://doi.org/10.1016/j.conbuildmat.2020.120156.
[44] L.P. Thives, J.C. Pais, P.A.A. Pereira, G. Trichês, S.R. Amorim, Assessment of the digestion time of asphalt rubber binder based on microscopy analysis, Constr. Build. Mater. 47 (2013) 431–440, https://doi.org/10.1016/j.conbuildmat.2013.05.087.
[45] EN 12697-29, Bituminous Mixtures - Test Method for Hot Mix Asphalt - Part 29: Determination of the Dimensions of Bituminous Specimen, 2002.
[46] H.U. Bahia, T.P. Friemel, P.A. Peterson, J.S. Russell, B. Poehnelt, Optimization of constructibility and resistance to traffic: a new design approach for HMA using the superpave compactor, J. Assoc. Asph. Paving Technol. 67 (1998).
[47] P. Mikhailenko, M.R. Kakar, Z. Piao, M. Bueno, L. Poulikakos, Improving the sustainability of semi-dense asphalt pavements by replacement of recycled concrete aggregate fractions, in: C. Raab (Ed.), Proc. 9th Int. Conf. Maint. Rehabil. Pavements—Mairepav9, Springer International Publishing, Cham 2020, pp. 343–351, https://doi.org/10.1007/978-3-030-48679-2_33.
[48] EN 12697-12, Bituminous Mixtures - Test Methods for Hot Mix Asphalt - Part 12: Determination of the Water Sensitivity of Bituminous Specimens, 2008.
[49] R. Roque, B. Birgisson, Z. Zhang, B. Sangpetngam, T. Grant, Implementation of SHRP Indirect Tension Tester to Mitigate Cracking in Asphalt Pavements and Overlays, University of Florida, Gainesville, FL, USA, 2002.
[50] P. Park, S. El-Tawil, S.-Y. Park, A.E. Naaman, Cracking resistance of fiber reinforced asphalt concrete at −20°C, Constr. Build. Mater. 81 (2015) 47–57, https://doi.org/10.1016/j.conbuildmat.2015.02.005.
[51] EN 12697-44, Bituminous Mixtures - Test Methods for Hot Mix Asphalt - Part 44: Crack Propagation by Semi-circular Bending Test, 2019.
[52] L.D. Poulikakos, S. dos Santos, M. Bueno, S. Kuentzel, M. Hugener, M.N. Partl, Influence of short and long term aging on chemical, microstructural and macromechanical properties of recycled asphalt mixtures, Constr. Build. Mater. 51 (2014) 414–423, https://doi.org/10.1016/j.conbuildmat.2013.11.004.
[53] Technische Prüfvorschriften für Asphalt: Einaxialer Druckschwellversuch - Bestimmung des Verformungsverhaltens von Walzasphalt bei Wärme2010.
[54] EN 12697-25, Bituminous Mixtures - Test Methods - Part 25: Cyclic Compression Test, 2019.
[55] P.L. Menezes, M. Nosonovsky, S.P. Ingole, S.V. Kailas, M.R. Lovell, Tribology for Scientists and Engineers: From Basics to Advanced Concepts, Springer Science & Business Media, 2013.
[56] V. Swami, V. Tandon, S. Nazarian, Mix Design Procedure for Crumb Rubber Modified Hot Mix Asphalt, University of Texas at El Paso. Center for Transportation Infrastructure, El Paso, TX, 2005.
[57] B.I. Siswosoebrotho, K. Ginting, Workability and resilient modulus of asphalt concrete mixtures containing flaky aggregates shape, J. East. Asia Soc. Transp. Stud. 6 (2005) 11.
[58] M.M. Rahman, G.D. Airey, A.C. Collop, Moisture susceptibility of high and low compaction dry process crumb rubber–modified asphalt mixtures, Transp. Res. Rec. J. Transp. Res. Board. 2180 (2010) 121–129, https://doi.org/10.3141/2180-14.
[59] M. Yu, G. Wu, J. Zhou, S. Easa, Proposed compaction procedure for dry process crumb rubber modified asphalt mixtures using air void content and expansion ratio, J. Test. Eval. 42 (2014) 20120337, https://doi.org/10.1520/JTE20120337.
[60] G. Dondi, P. Tataranni, M. Pettinari, C. Sangiorgi, A. Simone, V. Vignali, Crumb rubber in cold recycled bituminous mixes: comparison between traditional crumb rubber and cryogenic crumb rubber, Constr. Build. Mater. 68 (2014) 370–375, https://doi.org/10.1016/j.conbuildmat.2014.06.093.
[61] F.M. Soto, G.D. Mino, Increased stability of rubber modified asphalt mixtures to swelling expansion and rebound effect during post compaction, Transp. Veh. Eng. (2017) 1307–6892.
[62] US DOT, The Use of Recycled Tire Rubber to Modify Asphalt Binder and Mixtures, Office of Asset Management, Pavements, and Construction, Federal Highway Administration, US Department of Transportation, Washington, DC, 2014.
[63] Swiss Standard SN 640 431-1c-NA, Asphaltmischgut Mischgutanforderungen – Teil 1: Asphaltbeton, 2014.
[64] T. Baghaee Moghaddam, M. Soltani, M.R. Karim, Experimental characterization of rutting performance of polyethylene terephthalate modified asphalt mixtures under static and dynamic loads, Constr. Build. Mater. 65 (2014) 487–494, https://doi.org/10.1016/j.conbuildmat.2014.05.006.
[65] B. Singh, L. Kumar, M. Gupta, M. Chauhan, G.S. Chauhan, Effect of activated crumb rubber on the properties of crumb rubber-modified bitumen, J. Appl. Polym. Sci. 129 (2013) 2821–2831, https://doi.org/10.1002/app.38991.
[66] R. Choudhary, A. Kumar, K. Murkute, Properties of waste polyethylene terephthalate (PET) modified asphalt mixes: dependence on PET size, PET content, and mixing process, Period. Polytech. Civ. Eng. 62 (2018) 685–693, https://doi.org/10.3311/PPci.10797.
[67] I. Aghayan, R. Khafajeh, Chapter 12 - recycling of PET in asphalt concrete, in: F. Pacheco-Torgal, J. Khatib, F. Colangelo, R. Tuladhar (Eds.), Use Recycl. Plast. Eco-Effic. Concr, Woodhead Publishing 2019, pp. 269–285, https://doi.org/10.1016/B978-0-08-102676-2.00012-8.
[68] N. Usman, M.I.M. Masirin, K.A. Ahmad, M. Nda, The use of plastic fiber for minimizing stripping potential of bituminous mixture, Int. J. Integr. Eng. 10 (2018) https://doi.org/10.30880/ijie.2018.10.09.021.
[69] L. Chu, T.F. Fwa, K.H. Tan, Evaluation of wearing course mix designs on sound absorption improvement of porous asphalt pavement, Constr. Build. Mater. 141 (2017) 402–409, https://doi.org/10.1016/j.conbuildmat.2017.03.027.
[70] Y. Ding, H. Wang, FEM-BEM analysis of tyre-pavement noise on porous asphalt surfaces with different textures, Int. J. Pavement Eng. 0 (2017) 1–8, https://doi.org/10.1080/10298436.2017.1388507.
[71] M. Li, W. van Keulen, E. Tijs, M. van de Ven, A. Molenaar, Sound absorption measurement of road surface with in situ technology, Appl. Acoust. 88 (2015) 12–21, https://doi.org/10.1016/j.apacoust.2014.07.009.
[72] S. Mun, Sound absorption characteristics of porous asphalt concrete pavements, Can. J. Civ. Eng. 37 (2010) 273–278, https://doi.org/10.1139/L09-142.
[73] A. Vaitkus, T. Andriejauskas, V. Vorobjovas, A. Jagniatinskis, B. Fiks, E. Zofka, Asphalt wearing course optimization for road traffic noise reduction, Constr. Build. Mater. 152 (2017) 345–356, https://doi.org/10.1016/j.conbuildmat.2017.06.130.
[74] H. Wang, Y. Ding, G. Liao, C. Ai, Modeling and optimization of acoustic absorption for porous asphalt concrete, J. Eng. Mech. 142 (2016) https://doi.org/10.1061/(ASCE)EM.1943-7889.0001037.
[75] E. Bühlmann, P. Bürgisser, T. Ziegler, C. Angst, T. Beckenbauer, Forschungspaket Lärmarme Beläge Innerorts Teilprojekt (TP) 3: Langzeitmonitoring, Bundesamt für Umwelt BAFU, Bundesamt für Strassen ASTRA, Switzerland, 2017.
[76] V.F. Vázquez, S.E. Paje, Study of the road surface properties that control the acoustic performance of a rubberised asphalt mixture, Appl. Acoust. 102 (2016) 33–39, https://doi.org/10.1016/j.apacoust.2015.09.008.
[77] S.E. Paje, M. Bueno, F. Terán, R. Miró, F. Pérez-Jiménez, A.H. Martínez, Acoustic field evaluation of asphalt mixtures with crumb rubber, Appl. Acoust. 71 (2010) 578–582, https://doi.org/10.1016/j.apacoust.2009.12.003.
[78] V.F. Vázquez, J. Luong, M. Bueno, F. Terán, S.E. Paje, Assessment of an action against environmental noise: acoustic durability of a pavement surface with crumb rubber, Sci. Total Environ. 542 (2016) 223–230, https://doi.org/10.1016/j.scitotenv.2015.10.102.
[79] R. Sohaney, R.O. Rasmussen, Pavement Texture Evaluation and Relationships to Rolling Resistance at MnRoad, Minnesota Department of Transportation, St. Paul, MN, USA, 2013.
[80] ISO 13473-2, Characterization of Pavement Texture by Use of Surface Profiles — Part 2: Terminology and Basic Requirements Related to Pavement Texture Profile Analysis, 2010.
[81] L.D. Poulikakos, S. Athari, P. Mikhailenko, Z. Piao, M.R.K. Kakar, M. Bueno, R. Pieren, K. Heutschi, Use of waste and marginal materials for silent roads, Proc. 23rd Int. Congr. Acoust., Aachen, Germany, 2019.
[82] A. Del Pizzo, L. Teti, A. Moro, F. Bianco, L. Fredianelli, G. Licitra, Influence of texture on tyre road noise spectra in rubberized pavements, Appl. Acoust. 159 (2020) 107080, https://doi.org/10.1016/j.apacoust.2019.107080.
[83] M. Losa, P. Leandri, M. Cerchiai, Improvement of pavement sustainability by the use of crumb rubber modified asphalt concrete for wearing courses, Int. J. Pavement Res. Technol. 5 (2012) 395–404.
[84] G. De León, A. Del Pizzo, L. Teti, A. Moro, F. Bianco, L. Fredianelli, G. Licitra, Evaluation of tyre/road noise and texture interaction on rubberised and conventional pavements using CPX and profiling measurements, Road Mater. Pavement Des. (2020) https://doi.org/10.1080/14680629.2020.1735493.

[85] M. Losa, P. Leandri, R. Bacci, Empirical rolling noise prediction models based on pavement surface characteristics, Road Mater. Pavement Des. 11 (2010) 487–506, https://doi.org/10.1080/14680629.2010.9690343.

[86] D.A. Mansura, N.H. Thom, H.J. Beckedahl, Numerical and experimental predictions of texture-related influences on rolling resistance, Transp. Res. Rec. 2672 (2018) 430–439, https://doi.org/10.1177/0361198118776114.

[87] P.A. Serigos, A. De Fortier Smit, J.A. Prozzi, Incorporating surface microtexture in the prediction of skid resistance of flexible pavements, Transp. Res. Rec. 2457 (2014) 105–113, https://doi.org/10.3141/2457-11.

[88] S.W. Goh, Z. You, Mechanical properties of porous asphalt pavement materials with warm mix asphalt and RAP, J. Transp. Eng. 138 (2012) 90–97, https://doi.org/10.1061/(ASCE)TE.1943-5436.0000307.